



ELSEVIER

Journal of Alloys and Compounds 337 (2002) 83–88

Journal of
ALLOYS
AND COMPOUNDS

www.elsevier.com/locate/jallcom

Crystallization kinetics of an amorphous $\text{Al}_{85}\text{Ni}_{10}\text{Y}_{2.5}\text{La}_{2.5}$ alloy

O.N. Senkov^{a,*}, J.M. Scott^a, D.B. Miracle^b^aUES, Inc., 4401 Dayton-Xenia Rd., Dayton, OH 45432-1894, USA^bAir Force Research Laboratory, Materials and Manufacturing Directorate, Wright Patterson AFB, OH 45433-7817, USA

Received 11 June 2001; received in revised form 13 September 2001; accepted 18 September 2001

Abstract

Amorphous $\text{Al}_{85}\text{Ni}_{10}\text{Y}_{2.5}\text{La}_{2.5}$ alloy powder with the particle size of -500 mesh was produced by gas atomization. Crystallization kinetics of the amorphous phase were studied using differential thermal analysis (DTA), X-ray diffraction (XRD), and scanning electron microscopy. Crystallization occurred in the temperature range $230\text{--}450^\circ\text{C}$ in three exothermic reaction steps. The onset and peak temperatures for these reactions shifted toward higher temperatures when the heating rate was increased; this allowed the activation energies of the mechanisms controlling each step of the crystallization to be determined as 148, 336, and 274 kJ/mol, respectively. XRD and SEM analysis of the powder heated to different temperatures showed that precipitation of Al-based particles occurred during the first exothermic reaction, crystallization of the Al_4La phase and an increase in the volume fraction of the Al-based phase took place during the second exothermic reaction, and development of the Al_3Ni phase occurred during the third exothermic reaction. After annealing at 550°C , the powder consisted of Al-based matrix reinforced with very fine intermetallic particles of different morphologies. The mechanism of crystallization is discussed. © 2002 Elsevier Science B.V. All rights reserved.

Keywords: Amorphous materials; Crystal growth; X-ray diffraction; Scanning electron microscopy; Thermal analysis

1. Introduction

High-strength and light-weight aluminum-based alloys have attracted rapidly increasing interest of scientists and manufacturers [1,2]. An upper strength limit of about $500\text{--}600$ MPa can be achieved in conventional aluminum alloys strengthened by conventional strengthening mechanisms, i.e. solid solution, grain size refinement, dispersion/precipitation, work hardening and/or fiber/particle reinforcement [3]. Producing far-from-equilibrium structures, such as amorphous or nanocrystalline structures, can increase the properties considerably [4–7]. Ultimate tensile strength exceeding 1000 MPa was reported for several Al-based amorphous alloys and maximum strength of 1560 MPa was achieved in specially designed aluminum alloys containing an amorphous matrix and dispersion of Al-based nano-particles [1]; although these data were obtained in thin ribbons.

Amorphous aluminum alloys are a relatively new class of materials containing ≥ 80 at.% Al, with the remainder consisting of a rare earth metal and transition metals [4,8].

A high critical cooling rate of above 10^4 °C/s is typically required to form a fully amorphous product in ribbon, flakes or powder forms, and special low-temperature compaction techniques are required to produce bulk parts, limiting potential applications. Unique microstructures can be produced by controlled crystallization of the fully amorphous product. In some systems, both strength and ductility increase in the partially crystalline state [1,4]. Other amorphous alloys produce intermetallic or quasicrystalline precipitates upon crystallization, providing a credible path for increasing the specific stiffness. From these points of view, study of the crystallization kinetics is very important to control compaction processes and to achieve good microstructure–property combinations.

In the present work, kinetics of crystallization in an amorphous $\text{Al}_{85}\text{Ni}_{10}\text{Y}_{2.5}\text{La}_{2.5}$ alloy powder was studied using a differential thermal analysis (DTA) technique complimented with X-ray diffraction (XRD) and scanning electron microscopy (SEM).

2. Experimental

Gas atomized (GA) -200 mesh powder of a nominal composition of 85Al, 10Ni, 2.5Y and 2.5La (in atomic

*Corresponding author. Tel.: +1-937-255-1320; fax: +1-937-656-7292.

E-mail address: oleg.senkov@wpafb.af.mil (O.N. Senkov).

Table 1
Actual chemical composition of the gas atomized powder

Element	Al	Ni	La	Y	Fe	Mo	O	N	C
Concentration (wt.%)	Base	16.86	10.37	6.46	0.23	<0.05	0.372	<0.003	0.025

percents) was supplied by DWA Al Composites, Chatsworth, CA. High purity helium at a pressure of 690 MPa was used for atomization. The actual chemical composition of the powder is given in Table 1. The powder was sieved into three grades with particle sizes -500 mesh ($\leq 23 \mu\text{m}$), $-325/+500$ mesh ($\leq 38 \mu\text{m}/>23 \mu\text{m}$), and $-200/+325$ mesh ($\leq 70 \mu\text{m}/>38 \mu\text{m}$). Microstructural analysis showed that the -500 mesh powder was essentially amorphous, although single crystalline dendrites were present in some particles. The powder of $-200/+325$ mesh size was fully crystalline, and the intermediate grade powder ($-325/+500$ mesh) was less than 40% amorphous, containing crystalline dendrites in an amorphous phase, Fig. 1. Crystallization kinetics of the amorphous phase were studied in the -500 mesh powder. DTA was

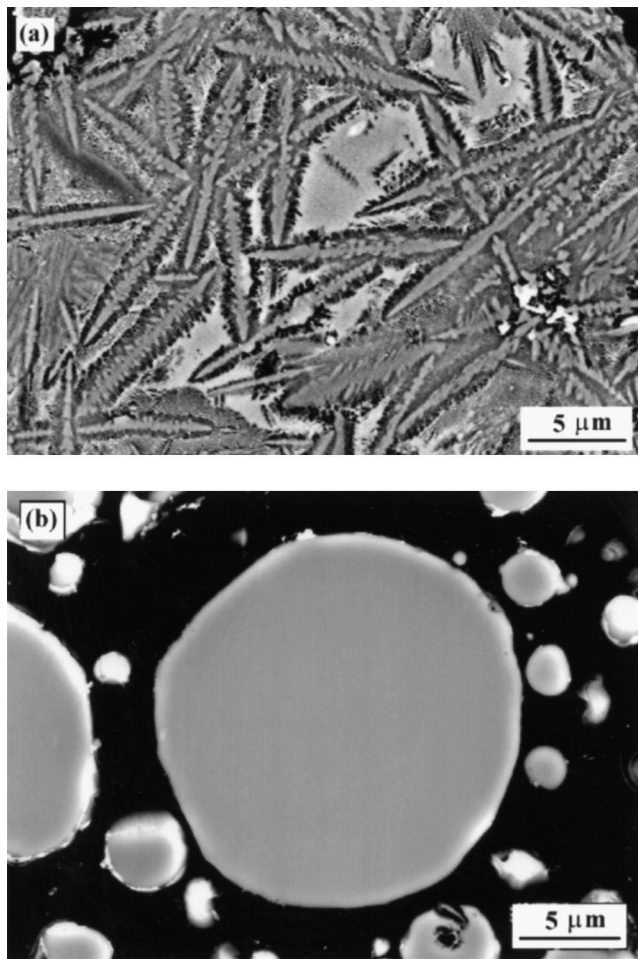


Fig. 1. SEM back-scattering images of cross-sections of the powder particles of different size grades: (a) $-200/+325$ mesh, (b) -500 mesh.

performed on heating in the temperature range of 50–650°C in an argon atmosphere using a Universal V2.3C TA unit. Heating rates of 5, 10, 20 and 50°C/min were used to determine the activation enthalpy of the processes controlling crystallization by Kissinger's method [9,10]. Heat of reactions was determined using a differential scanning calorimeter DSC Q1000 V2.45 at a heating rate of 20°C/min. Microstructural characterization was performed on powder heated to a selected temperature with the rate of 10°C/min and then immediately cooled with the rate exceeding 20°C/min. The phases present in the powder were examined with the use of a Rigaku Rotaflex X-ray diffractometer and a Leica 360FE scanning electron microscope.

3. Results

3.1. Thermal analysis

Fig. 2 shows DTA curves of the gas atomized powder. The curves were obtained at four different heating rates. Three exothermic peaks corresponding to crystallization of an amorphous phase are observed in the temperature range of 230–450°C. The crystallization begins at a higher temperature and the onset and peak temperatures for the exothermic reactions responsible for the crystallization are shifted toward higher temperatures when the heating rate is increased. The values for the onset and peak temperatures are tabulated in Table 2. It can be seen that the temperature for the onset of initial crystallization, T_x , increases from

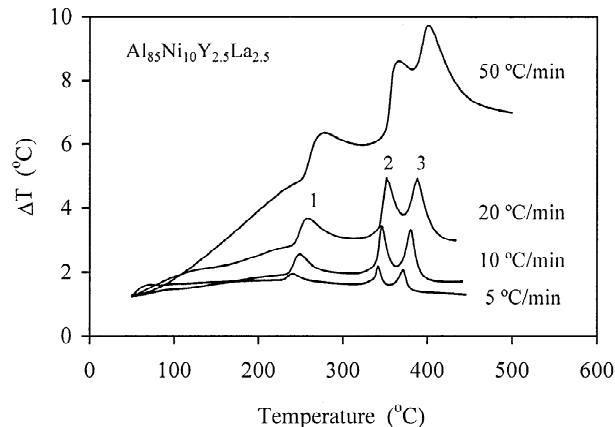


Fig. 2. DTA curves of an $\text{Al}_{85}\text{Ni}_{10}\text{Y}_{2.5}\text{La}_{2.5}$ amorphous powder at different heating rates.

Table 2

Onset and maximum temperatures of the exothermic reactions for crystallization at different heating rates

Heating rate (°C/min)	First peak		Second peak		Third peak	
	Onset (°C)	Peak (°C)	Onset (°C)	Peak (°C)	Onset (°C)	Peak (°C)
5	230.8	240.5	336.0	341.6	361.9	371.4
10	237.0	248.6	339.3	346.2	369.2	380.3
20	243.2	257.0	342.2	351.7	376.1	388.3
50	253.9	274.6	352.7	362.8	387.7	400.8

231 to 254°C when the heating rate increases from 5 to 50°C/min.

According to Kissinger [9], the activation energy, E , of the process controlling the transformation is given by the following equation:

$$E = -R d[\ln(v/T_p^2)]/d(1/T_p) \quad (1)$$

where v is the heating rate, T_p is the peak maximum temperature, and R is the gas constant. Therefore, the activation energy can be determined from slopes of the curves $\ln(v/T_p^2)$ versus $1/T_p$; these curves plotted in Fig. 3 for each of the three exothermic reactions show linear dependencies. The activation energies were determined for the first, second and third crystallization peaks to be 148, 336, and 274 kJ/mol, respectively, Table 3.

The heat of reactions, ΔH , was determined using DSC, and the ΔH values are given in Table 3. One can see that the heats of the second and third reactions (22.6 and 27.2 J/g, respectively) are more than 1.5 times higher than the heat of the first reaction (14.5 J/g).

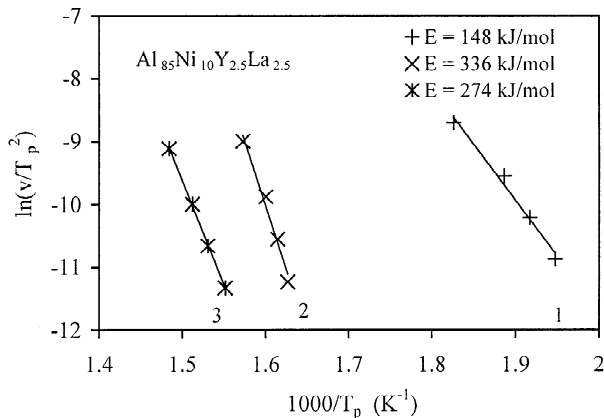


Fig. 3. Dependencies of the logarithm of the heating rate (in K/min) normalized to the square of the peak temperature T_p on the reciprocal peak temperature for the first, second and third exothermic peaks.

Table 3

Activation energy, E , and heat of reaction, ΔH , corresponding to the three crystallization peaks

Peak no.	1	2	3
E , kJ/mol	148	336	274
ΔH , J/g	14.5	22.6	27.2

3.2. Phase and microstructural analysis

3.2.1. X-ray diffraction

X-ray diffraction patterns of the -500 -mesh $\text{Al}_{85}\text{Ni}_{10}\text{Y}_{2.5}\text{La}_{2.5}$ powder in the as-GA condition and after annealing at different temperatures are shown in Fig. 4. A spread halo (in the 2θ range of 30 – 50°) from an amorphous phase and separate peaks from three crystalline phases, Al, Al_3Ni and Al_4La , were detected in the as-GA condition. The positions of Al peaks were shifted in the range of lower angles indicating the lattice expansion due to solid solution of Y and/or La. After heating to a temperature of 290°C , i.e. just between the first and second exothermic reactions, the halo intensity decreased, the intensities of Al peaks increased and the intensities of peaks from other phases remained almost unchanged, Fig. 4b, suggesting that the first exothermic reaction was caused by precipitation of the fcc Al phase from the amorphous matrix.

Annealing of the powder at a temperature of 360°C , just above the second exothermic reaction and below the third reaction, led to further decrease in the intensity of the halo and increase in the intensity of peaks from Al phase and,

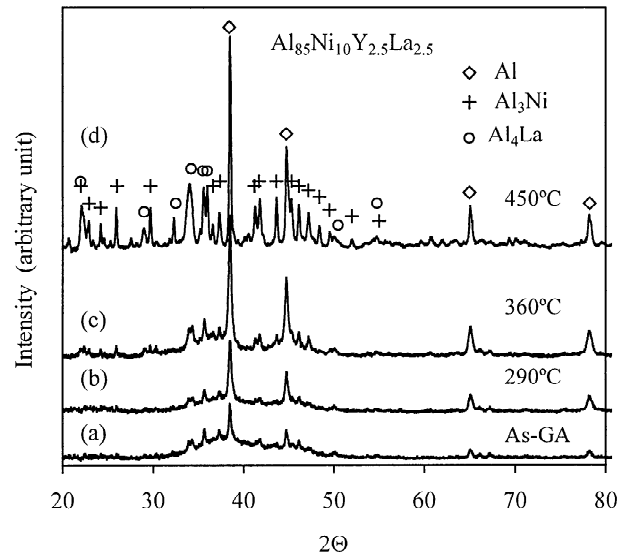


Fig. 4. X-ray diffraction patterns of the $\text{Al}_{85}\text{Ni}_{10}\text{Y}_{2.5}\text{La}_{2.5}$ gas atomized powder in (a) as-received condition and after heating to (b) 290°C , (c) 360°C , and (d) 450°C with a heating rate of $10^\circ\text{C}/\text{min}$. The powder is $<23 \mu\text{m}$ in size.

additionally, to an increase in intensities of peaks from the Al_4La intermetallic phase, Fig. 4c. One may therefore conclude that crystallization of the Al_4La phase, along with further increase in the volume fraction of the Al phase, is responsible for the second exothermic reaction. When the powder was heated to a temperature above the third exothermic reaction (450°C in Fig. 4d), the crystallization was completed and the XRD peaks from at least three phases, Al, Al_3Ni , and Al_4La , were well defined on the corresponding X-ray diffraction pattern. During this stage, crystallization of the Al_3Ni phase was the major event, although intensities of the peaks from other phases also increased.

With an increase in the annealing temperature, the lattice parameter of the fcc Al phase decreased from $a=0.4053$ nm in as-GA powder to $a=0.4049$ in the powder annealed at 450°C . The latter value is very close to the lattice

parameter of pure Al [11]. Evolution of particle sizes of Al and intermetallic phases was estimated from analysis of widths of corresponding XRD peaks. In the as-GA powder the average size of crystalline Al particles was estimated to be 103 nm. After annealing at 290°C , it decreased to 57 nm, indicating precipitation of new smaller particles, and after annealing at 390°C the size of Al particles increased to 125 nm. After annealing at 450°C , the size of intermetallic particles was ~ 95 nm and the size of Al grains ~ 200 nm.

3.2.2. Scanning electron microscopy

No microstructural features were detected on the cross-sections of the powder particles after annealing at 290°C , similar to Fig. 1b. After annealing at 390°C , very fine irregular-shaped particles were observed, Fig. 5a, and after

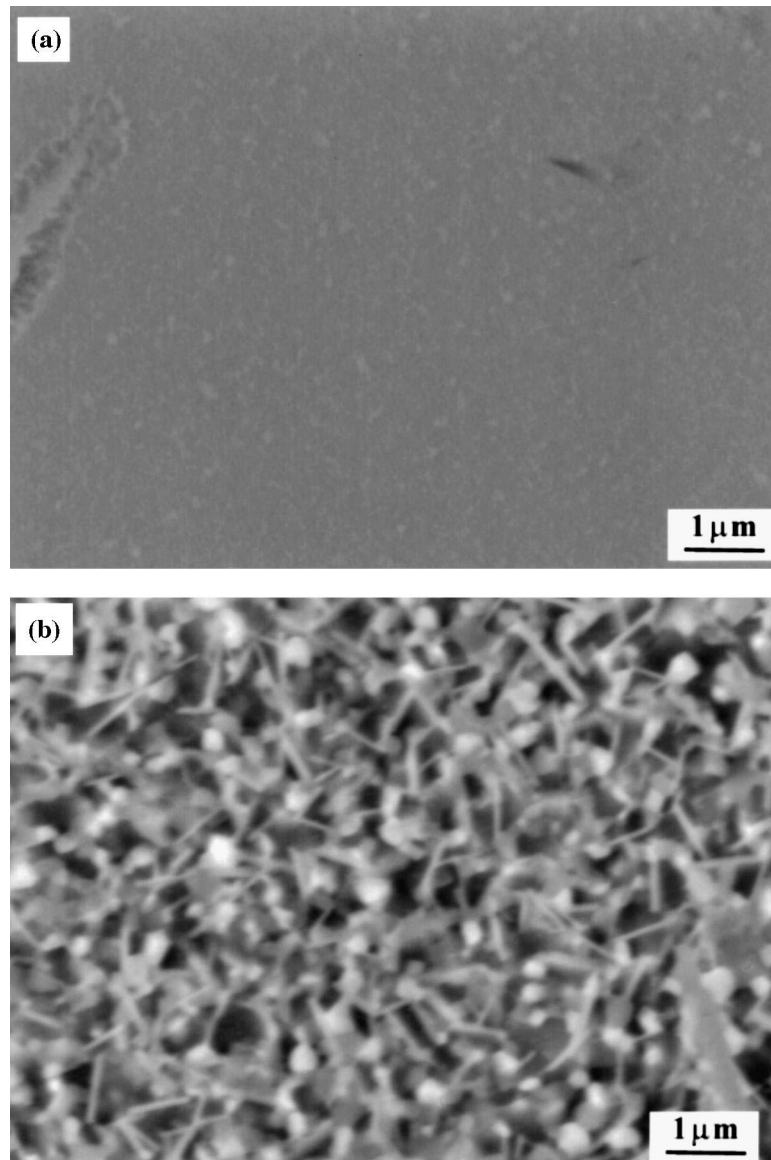


Fig. 5. SEM back-scattering images of cross-sections of the powder particles after annealing at (a) 390°C and (b) 550°C .

annealing at 550°C, particles of at least two morphologies, spherical and needle-like, were distinguished, Fig. 5b.

4. Discussion

The present results show that an amorphous alloy powder of the composition of $\text{Al}_{85}\text{Ni}_{10}\text{Y}_{2.5}\text{La}_{2.5}$ can be produced by gas atomization. The powder particles with a size less than 23 μm are predominantly amorphous and the powder particles with a size larger than 38 μm are fully crystalline. This result indicates that a high cooling rate, $\geq 10^4$ °C/s, is required to amorphize the alloy. Similar critical cooling rate was estimated for an $\text{Al}_{85}\text{Ni}_{10}\text{Ce}_5$ amorphous alloy produced in the form of wire (~50 μm in diameter) or melt-spun ribbon (~15 μm thick) [4]. The amorphous phase in the $\text{Al}_{85}\text{Ni}_{10}\text{Y}_{2.5}\text{La}_{2.5}$ alloy is stable on heating to a temperature of about 230°C. Above this temperature, crystallization occurs in three steps resulting in three exothermic reactions with different onset temperatures and kinetics. The first exothermic reaction, which is observed in the temperature range 230–270°C (at a heating rate of 10°C/min), is due to precipitation of the fcc Al phase in the amorphous matrix. This process decreases the average size of crystalline particles from 103 nm in as-produced powder to 57 nm in the powder heated to 290°C. The activation energy of the first reaction, $E_1 = 148$ kJ/mol, is close to the self-diffusion activation energy of aluminum [12], indicating that the Al-phase precipitation is probably controlled by the self diffusion of aluminum. Because of low solubility of Ni, Y and La in the fcc Al phase, the remnant amorphous phase becomes enriched with the alloying elements, especially near the aluminum particles. These increased concentrations stabilize the amorphous phase and hinder crystallization [13,14]; despite the strongly exothermic crystallization reaction, with a heat of reaction of $\Delta H = 14.5$ J/g. The crystallization continues further only after increasing the temperature to about 330°C. This may indicate that higher nominal concentrations of alloying elements are required to stabilize the amorphous phase and increase the crystallization temperature T_x . However, the increasing concentrations would increase the melting temperature of the alloy very rapidly, which would decrease the glass-forming ability during melt quenching [8,15].

The second step of devitrification of the amorphous phase occurs in the temperature range 330–360°C and leads to crystallization of the Al_4La phase. The high activation energy of the reaction ($E_2 = 336$ kJ/mol) indicates that diffusion of lanthanum controls crystallization during this stage. A decrease in the concentration of lanthanum in the amorphous phase destabilizes the remnant amorphous phase and leads to an increase in the volume fraction of the fcc aluminum phase and formation of the Al_3Ni phase. The latter process is responsible for the third exothermic reaction in the temperature range of 360–450°C with the activation energy $E_3 = 274$ kJ/mol.

This value corresponds to the activation energy of diffusion of nickel in the aluminum matrix [12]. The absence of an yttrium-containing intermetallic phase may indicate that this element is dissolved in the Al_4La and/or Al_3Ni phases.

5. Conclusions

Essentially amorphous powder with a size less than 23 μm was produced from an $\text{Al}_{85}\text{Ni}_{10}\text{Y}_{2.5}\text{La}_{2.5}$ alloy by gas atomization. The amorphous phase was stable on heating to a temperature of about 230°C and then crystallization occurred in three stages. Initially, in the temperature range 230–270°C, an fcc aluminum phase precipitated as fine particles in the amorphous phase; the process controlled by diffusion of aluminum with the activation energy $E_1 = 148$ kJ/mol. An increased content of the alloying elements stabilized the remnant amorphous phase and crystallization continued only after increasing the temperature above 330°C. In the temperature range 330–360°C, an Al_4La phase was formed. The activation energy $E_2 = 336$ kJ/mol was measured indicating that diffusion of lanthanum controlled this transformation stage. During the final, third stage of crystallization, which occurred in the temperature range of 360–450°C, an Al_3Ni phase was developed and the activation energy was $E_3 = 274$ kJ/mol. After the completion of the crystallization, the alloy consisted of three major phases, Al, Al_3Ni and Al_4La with an average size of intermetallic particles of about 95 nm and a grain size of the aluminum matrix of about 200 nm.

Acknowledgements

The work was supported by the Air Force Research Laboratory under contract no. F33615-96-C-5258. The authors are thankful to DWA Al Composites, Inc., Chatsworth, CA for providing the amorphous powder. Discussions with Prof. J. Perepezko, Dr. J. Spowart and Dr. K. Kendig are appreciated.

References

- [1] A. Inoue, H. Kimura, Mater. Sci. Eng. A286 (2000) 1–10.
- [2] E.L. Courtright, S. Baskaran, D.A. Nelson, H.C. Reid, Materials for Advanced Rocket Propulsion — an Assessment of Materials and Process Development Needs, PNNL, Edwards, AFB, 1996, WL-TR-96-4086.
- [3] H. Jones, Alum. Alloys 54 (1978) 274.
- [4] A. Inoue, Prog. Mater. Sci. 43 (1998) 365–520.
- [5] F.H. Froes, P.D. Desai, Recent developments in powder metallurgy processing techniques, in: MIAC Report #5, DoD CINDAS, West Lafayette, IN, 1994.
- [6] O.N. Senkov, F.H. Froes, V.V. Stolyarov, R.Z. Valiev, Nanostruct. Mater. 10 (1998) 691–698.
- [7] H. Kimura, L. Wang, A. Inoue, Mater. Trans. JIM 39 (8) (1998) 866–869.

- [8] F.Q. Guo, S.J. Poon, G.J. Shiflet, *Mater. Sci. Forum* 331–337 (2000) 31–42.
- [9] H.E. Kissinger, *Anal. Chem.* 29 (1957) 1702–1705.
- [10] W.W.M. Wendlandt, in: 3rd Edition, *Thermal Analysis*, John Wiley, New York, 1980.
- [11] *International Tables for X-Ray Crystallography*, Birmingham, UK, 1968.
- [12] H.I. Aaronson (Ed.), *Diffusion*, ASM, Metals Park, OH, 1973.
- [13] W.S. Sun, M.X. Quan, *Mater. Lett.* 27 (1996) 101–105.
- [14] D.R. Allen, J.C. Foley, J.H. Perepezko, *Acta Mater.* 46 (1998) 431–440.
- [15] P.R. Okamoto, N.Q. Lam, L.E. Rehn, in: H. Ehrenreich, F. Spaepen (Eds.), *Solid State Physics: Advances in Research and Applications*, Vol. 52, Academic Press, NY, 1999, pp. 1–135.